Controlling factors of chorus spectral gaps 1 2 Jinxing Li^{1*} (http://orcid.org/0000-0003-0500-1056) 3 Jacob Bortnik¹ (https://orcid.org/0000-0001-8811-8836) 4 Wen Li² (https://orcid.org/0000-0003-3495-4550) 5 Xin An³ (http://orcid.org/0000-0003-2507-8632) 6 Larry R. Lyons¹ (https://orcid.org/0000-0002-9867-3638) 7 William S. Kurth⁵ (http://orcid.org/0000-0002-5471-6202) 8 George B. Hospodarsky⁵ (http://orcid.org/0000-0001-9200-9878) 9 David P. Hartley⁵ (https://orcid.org/0000-0001-8630-8054) 10 Geoffrey D. Reeves^{6,7} (https://orcid.org/0000-0002-7985-8098) 11 Herbert O. Funsten⁸ (https://orcid.org/0000-0002-6817-1039) 12 J. Bernard Blake⁹ (https://orcid.org/0000-0001-7439-4362) 13 Harlan Spence¹⁰ (https://orcid.org/0000-0002-2526-2205) 14 Daniel N. Baker¹¹ (https://orcid.org/0000-0001-5909-0926) 15 16 ¹Department of Atmospheric and Oceanic Sciences, University of California, Los Angeles, 17 California, 90095, USA 18 19 ²Center for Space Physics, Boston University, Boston, Massachusetts, 02215, USA 20 ³Department of Atmospheric and Oceanic Sciences and Department of Earth, Planetary, and 21 Space Sciences, University of California, Los Angeles, Los Angeles, California, 90095, USA 22 ³Laboratory For Atmospheric and Space Physics, University of Colorado, Boulder, Colorado 23 80303, USA ⁴School of Physics and Astronomy, University of Minnesota, Minnesota, Minnesota, 55455, 24 25 **USA** 26 ⁵Department of Physics and Astronomy, University of Iowa, Iowa City, Iowa, 52242-1479, USA ⁶Space Science and Applications Group, Los Alamos National Laboratory, Los Alamos, New 27 Mexico, 87544, USA 28

⁸The New Mexico Consortium, Los Alamos, New Mexico, 87544, USA

⁷Los Alamos National Laboratory, MS-D466, PO Box 1663, Los Alamos, New Mexico, 87545,

29

30

31

USA

- ⁹Space Science Applications Laboratory, The Aerospace Corporation, El Segundo, California,
- 33 90245, USA
- 34 ¹⁰Institute for the Study of Earth, Oceans, and Space, University of New Hampshire, Durham,
- 35 New Hampshire 03824-3525, USA
- 36 ¹¹Laboratory for Atmospheric and Space Physics, University of Colorado, Boulder, Colorado
- 37 80303-7814, USA
- *Corresponding Author: Jinxing Li (jinxing.li.87@gmail.com)

40

Key Points

- 41 1) Freshly injected anisotropic electron population without a PSD plateau generates single band
- 42 chorus waves
- 2) Banded chorus waves are more common because electrons usually have already undergone
- 44 isotropization at Landau resonant energies along the drift path
- 45 3) Landau acceleration extending to higher energies occurring at higher latitudes leads to more
- 46 pronounced electron isotropization and larger chorus spectral gaps

47 Abstract

- 48 The present study compares a single-band chorus wave against a banded chorus wave observed
- 49 by Van Allen Probes at adjacent times, and demonstrates that the single-band chorus wave is
- 50 associated with an anisotropic electron population over a broad energy range, while the banded
- 51 chorus wave is accompanied by an electron phase space density plateau and an electron
- 52 anisotropy reduction around Landau resonant energies. We further compare banded chorus
- waves with different spectral gap widths, and show that a wider spectral gap is associated with
- 54 electron isotropization extending to higher energies with respect to the equatorial Landau
- resonant energy. We suggest that early generated chorus waves isotropize electrons via Landau
- resonant acceleration, and the waves that propagate to higher latitudes isotropize electrons at
- 57 higher energies. The isotropization extending to higher energies leads to a larger spectral gap of
- new chorus waves after electrons bounce back to the equator.

Plain Language Summary

Naturally occurring chorus waves in the Earth's magnetosphere typically consist of two frequency bands. The present study aims to explain what controls the bandwidth of the chorus frequency gap that separates chorus waves into two bands. We first compare a single-band chorus wave against a banded chorus wave observed by a Van Allen Probe satellite at adjacent times. The banded chorus wave is accompanied by an electron phase space density plateau and an electron anisotropy reduction due to Landau resonance, while this phenomenon is not clearly seen in association with the single-band chorus wave. We further compare banded chorus waves with different gap widths. Satellite observations indicate that a wider frequency gap is associated with electron isotropization extending to higher energies. We suggest that Landau resonant acceleration extending to high latitudes isotropizes electron distribution at high energies, leading to new chorus waves with a large frequency gap. In contrast, Landau resonance that stops at a relatively lower latitude (due to waves being damped) leads to new chorus waves with a smaller frequency gap.

1. Introduction

74

75 Chorus waves in the Earth's magnetosphere are typically observed with a spectral gap around half of the equatorial f_{ce} (electron gyro-frequency), which separates the waves into an upper-band 76 77 and a lower-band (e.g., Tsurutani and Smith, 1974; Santolik et al., 2003). Single-band chorus waves that do not have a spectral gap or a significant intensity reduction around $0.5 f_{ce}$ have also 78 been observed (e.g., Kurita et al., 2012), but are less common than banded chorus waves. Van 79 Allen Probe burst-mode observations from 2012 to 2016 show that single-band chorus waves are 80 81 mostly observed on the Earth's morning side and the dayside (Teng et al., 2019), while banded 82 chorus waves have higher occurrences between midnight and dawn. THEMIS burst-mode observations from 2008 to 2015 show that banded chorus waves have an average spectral gap 83 width of $\sim 0.07 f_{ce}$, which is nearly independent of magnetic latitude (MLAT) and magnetic local 84 time (MLT) while having a weak dependence on L-shell (Gao et al., 2019). 85 86 Previous explanations for chorus gaps can be categorized into two scenarios: 1) chorus gaps are 87 formed as the waves propagate away from the equator to higher latitudes (e.g., Tsurutani & Smith, 1974; Omura et al., 2009; 2020; Bortnik et al., 2006); 2) chorus gaps, including those 88 formed due to nonlinear mechanisms (Schriver et al., 2010; Gao et al., 2016), are observed in the 89 source region (e.g., Liu et al., 2011; Fu et al., 2014; Ratcliffe and Watt, 2017; Li et al., 2019a). Li 90 91 et al., (2022) showed banded chorus waves consisting of interleaved parallel and anti-parallel elements near the equator, revealing that chorus gaps are formed in the equatorial source region, 92 93 instead of being developed as the waves propagate to high latitudes. This is consistent with the statistical results that banded chorus waves are mostly observed within ~6° in MLAT, while 94 95 single-band chorus waves are observed over a slightly wider MLAT range, instead of being closer to the equator (Gao et al., 2019; Teng et al., 2019). 96 Chorus spectral gaps are usually observed below the equatorial $0.5 f_{ce}$, and the upper-band 97 98 usually arises very nearly from the 0.5 fce frequency (Tsurutani and Smith, 1974; Burtis and Helliwell, 1976; Santolik et al., 2003; Fu et al., 2014; Gao et al., 2019; Teng et al., 2019). 99 100 Banded chorus waves in the Jovian (Coroniti et al., 1980) and Saturnian magnetospheres (Hospodarsky et al., 2008) also show similar features with spectral gaps below 0.5 f_{ce}. Li et al. 101 102 (2019a; 2022) explained that chorus waves generated early in the process quickly cause parallel electron acceleration at Landau resonant velocities, which are around 0.5 v_{Ae} and increase with 103

increasing latitude. The Alfvenic velocity v_{Ae} , defined as $B/\sqrt{\mu_0\rho_e}$, or equivalently $c \cdot f_{ce}/f_{pe}$.

Here B is the ambient magnetic field strength, μ_0 is the magnetic permeability of free space, ρ_e is the electron density, c is the light speed in vacuum and f_{pe} is the electron plasma frequency.

The modified electron distribution is then reflected to the equator by the mirror force, forming a

PSD plateau and a reduced anisotropy above 0.5 v_{Ae} . The isotropized population suppresses the

chorus excitation just below $0.5 f_{ce}$, while the anisotropic populations not impacted by Landau

resonances generate new chorus waves at the lower- and upper-bands.

The spectral gap widths of banded chorus waves vary case by case, and as discussed in sections 2 and 3 in this paper, the gap width can vary significantly within a short time or over a small spatial scale. The present study aims to investigate important factors that determines the width of chorus spectral gaps, and under which conditions we might expect to observe a large gap. We will focus on in situ measurements in the source region near the equator identified by the coexistence of parallel and anti-parallel chorus waves. This is because satellites away from the equator cannot capture particle distributions at large equatorial pitch angles. More importantly, the quasi-parallel propagating chorus waves statistically propagate at wave normal angles centered around ~10°–15° (*Taubenschuss et al.*, 2016) near the equator and become more oblique at high latitudes, thus, the waves and particles measured away from equator may not originate from the same source region at the equator.

2. Single-band and two-band chorus waves

Li et al., (2022) investigated the 8 May 2016 event in which the two Van Allen Probes (Mauk et al., 2013) measured banded chorus waves near the source region over a period of several hours. The present study revisits this event from the perspective of understanding the controlling factors of the spectral gap width. Figure 1 presents the wave measurements provided by the waveform receiver (WFR) of the Waves instrument, which is part of the Electric and Magnetic Field Instrument Suite and Integrated Science (EMFISIS) suite (Kletzing et al., 2013), and the electron distribution provided by the Helium, Oxygen, Proton, and Electron (HOPE) instrument (Funsten et al., 2013), which is part of the Energetic Particles, Composition, and Thermal Plasma (ECT) suite (Spence et al., 2013). Figure 1a exhibits the burst-mode wave magnetic spectral intensity measured by Probe B at 07:31 UT, showing banded chorus waves with a gap around 0.5 f_{ce} and a gap width that varied between ~ 0.025 f_{ce} and ~ 0.05 f_{ce} . The waves measured at 07:42 UT,

presented in Figure 1d, show a mixture of single-band and banded with tiny gaps. The wave normal angle information calculated using the Means (1972) method, shown in Figures 1b and 1e, indicates that the banded chorus waves have small wave normal angles (~0°-45°) relative to the background magnetic field, and the waves shown in Figure 1e are more parallel to the background magnetic field. The Poynting flux angle with respect to the magnetic field, presented in Figures 1c and 1f, respectively, shows a coexistence between parallel and anti-parallel propagating elements, especially at the lower band, implying that the spacecraft was in the source region of chorus waves. Figure 1g shows the electron PSD distribution averaged over 07:30-07:33 UT, in association with the banded chorus wave. The f_{pe}/f_{ce} ratio, provided by the high-frequency receiver (HFR) and the magnetometer of the EMIFSIS suite, varied from 4 to 5 during this period. A PSD plateau is observed at 2.7 keV at 18° pitch angle and is close to a parallel velocity of $0.5 v_{Ae}$ calculated using $f_{pe}/f_{ce}=5$, suggesting a Landau resonant acceleration starting at the equator. The distribution at 18° pitch angle approaches that at 36° pitch angle at 3-6 keV, implying a reduced anisotropy possibly caused by Landau resonant acceleration at high latitudes. In contrast, the electron distribution averaged over 07:41-07:44 UT accompanied by the single-band chorus wave, shown in Figure 1h, does not exhibit a PSD plateau around 0.5 v_{Ae} , and the reduction of anisotropy is not evident. It is possible that the wave-particle interaction was at the initial stage, and only a small portion of electrons at $0.5 v_{Ae}$ were accelerated; therefore, chorus waves were a mixture of two-band and single-band elements. While banded chorus waves displayed in Figure 1a show a small frequency gap ($\sim 0.03 f_{ce}$), chorus waves are typically observed with significantly larger frequency gaps (Gao et al., 2019), which are typically accompanied with more pronounced PSD plateau extending to higher energies (Li et al., 2019a; 2022; also refer to the cases shown in Figures 2d and 4b). Those pronounced PSD plateaus are formed possibly because electrons around 0.5 v_{Ae} have undergone continuous isotropization along the drift path via Landau resonant interactions with chorus waves. As the two anisotropic electron populations drift inward due to the convection electric field or through a radial diffusion, they are preferentially energized in the direction perpendicular to the

134

135

136

137

138139

140

141

142

143

144

145

146

147

148

149

150

151

152

153

154

155

156

157

158

159

160

161

162

163

magnetic field. As a result, their anisotropy increases, providing free energy to continue

generating banded chorus waves in new locations. Banded chorus waves are more common than

single-band chorus waves, probably because energetic electrons form two anisotropic distributions by chorus waves all the way along their drift path. Single band chorus waves are possibly observed at locations where chorus waves are just beginning to be generated, and the electron isotropization due to Landau resonance has not yet taken place.

3. Expansion of chorus spectral gap width

To further explore the factors controlling the width of the chorus gap, we investigate chorus waves with an expanding spectral gap. Figures 2a and 2d show burst-mode wave spectra measured by Probe A starting from 09:26 UT and 09:33 UT, respectively. The two groups of chorus waves show similar wave normal angle characteristics (Figures 2b and 2e), and they were both in the source region, as identified by the alternating, oppositely directed Poynting flux angles (Figures 2c and 2f). However, the waves at 09:33 UT have a much wider spectral gap than the waves at 09:26 UT. The electron distribution associated with chorus at 09:26 UT, presented in Figure 2g, shows a PSD plateau around the equatorial 0.5 v_{Ae} (1.3 keV), and an isotropization up to ~3.3 keV. In contrast, the electron distribution associated with chorus waves at 09:33 UT, presented in Figure 2h, shows a broad plateau and isotropization up to ~4.1 keV, and $f(18^\circ)$ largely exceeded $f(36^\circ)$ in the range of 3.3-4.1 keV (the two dashed lines). This comparison demonstrates that the expansion of chorus gap is associated with pronounced parallel acceleration extending to higher energies.

Along the dipole magnetic held from the equator toward the pole, the magnetic field strength increases faster than the plasma density does; therefore, the Landau resonant velocity, which is associated with 0.5 v_{Ae} , increases as a function of latitude ($Li\ et\ al.$, 2019a). The isotropization above equatorial 0.5 v_{Ae} is most likely due to Landau resonant acceleration occurring at high latitudes. To estimate the latitudinal extent of the Landau resonance, we use a dipole magnetic field model and an empirical density model that $n \propto 1/\cos^{\alpha}\lambda$ (Denton et al., 2004) where we adopt a median value $\alpha = 2.8$. Even though chorus waves may become oblique when propagating to high latitudes, the largest possible Landau resonant velocity from all frequencies is still 0.5 v_{Ae} and roughly independent of the wave normal angle. This is because under the high density approximate ($\omega_{ce} \ll \omega_{pe}$), the reflective index is given by (Gurnett and Bhattacharjee, 2005)

$$n^2 = \frac{\omega_{pe}^2}{\omega(\omega_{ce}\cos\theta - \omega)}$$

where θ is the wave normal angle. The reflective index n minimizes at $2\omega_{pe}/(\omega_{ce}\cos\theta)$, which occurs at the frequency of $0.5~\omega_{ce}\cos\theta$. Hence, the largest possible Landau resonant velocity, $c/n\cos\theta$ is $0.5~v_{Ae}$. Using this fact, the acceleration at 3.3 keV for 18° pitch angle particles observed at 09:26 UT suggests a Landau resonant acceleration that occurred at latitudes up to ~21°. The acceleration at 4.1 keV observed at 09:33 UT indicates pronounced Landau resonant acceleration at latitudes up to ~23°.

We use the linear growth theory (*Kennel*, 1966) to quantitatively explain the generation and the expansion of the chorus gap due to enhanced parallel acceleration. Since the electron distributions are close to the power-law distribution, we use a combination of the kappa distribution and the Gaussian distribution to model the electron distributions, which are expressed as

$$f = \frac{n_0 2^{2\kappa - 1} (\kappa - 1/2) \Gamma^2(\kappa)}{\pi^2 \sqrt{\kappa} \Gamma(2\kappa) v_{T\perp}^2 v_{T\parallel}} \left(1 + \frac{v_{\perp}^2}{\kappa v_{T\perp}^2} + \frac{(v_{\parallel} - v_b)^2}{\kappa v_{T\parallel}^2} \right)^{-\kappa - 1},$$

$$f = \frac{n_0}{\pi^{3/2} v_{T\perp}^2 v_{T\parallel}} \left(-\frac{v_{\perp}^2}{v_{T\perp}^2} - \frac{(v_{\parallel} - v_b)^2}{v_{T\parallel}^2} \right).$$

Here $(v_{\perp}, v_{\parallel})$ are the particle velocities in the transverse and parallel directions with respect to the background magnetic field, and $(v_{T\perp}, v_{T\parallel})$ the perpendicular and parallel thermal velocities. The beam velocity is represented by v_b , and n_0 is the number density. The κ index is the exponent of the Kappa distribution at high energies, and the expression $\Gamma(\kappa)$ is the Gamma function. Min et al. (2015) suggested that accurately fitting the observed distribution using 19 components yields a result similar to that achieved using much fewer components. To simplify the scenario and avoid distractions, we conduct an experiment where the electron distribution consists of a cold isotropic component and a warm anisotropic component. The parameters for each component are listed in Table 1. We note that the modeled electron anisotropy is larger than the observed values so that high-frequency waves can grow, which is a common approach. The f_{pe}/f_{ce} ratio is 7, similar to the case in Figure 2.

Distribution	Density (cm ⁻³)	$v_{T\perp}$ (km/s)	$v_{T\parallel}$ (km/s)	v_b (km/s)
Kappa, <i>κ</i> =2	7.3	300	300	0
Kappa, <i>κ</i> =3	0.7	8,900	5,500	0
Gaussian	n_b	12,000	6,000	22,000

Table 1. The electron components and parameters that are used to fit the averaged electron distribution observed by Probe A during 09:33-09:36 UT.

We use a beam population with a bulk velocity 22,000 km/s (and another beam population with an opposite bulk velocity for symmetry) to model the parallel acceleration effect. We carried out three experiments with different densities of the beam: 1) n_b =0, 2) n_b =0.001 cm-3, and 3) n_b =0.002 cm-3, representing non acceleration, a weak Landau resonant acceleration and an enhanced Landau resonant acceleration, respectively, and the resultant electron PSD distributions are shown in Figures 3a-3c. Figures 3d-3f demonstrate the calculated wave growth rates contributed by cyclotron and Landau resonance. The electron distribution without the beam can excite chorus waves covering 0.1-0.65 f_{ce} without a gap. By adding a weak beam to the distribution, the linear growth theory produces banded chorus waves with a narrow gap (Figure 3e). Adding a strong beam which represents enhanced parallel acceleration extending to more energies, the linear theory produces a wider gap (Figure 3f).

We note that in the real magnetosphere, the Landau resonant energy increases with latitude, and the electron isotropization typically extends to high energies like that shown in Figure 2h and in previous studies (*Li et al.*, 2022), and the chorus gaps usually expend toward lower frequencies.

It is expected that chorus waves with very large spectral gaps are created by two anisotropic electron populations that are widely separated, in association with Landau resonant acceleration extending to very high velocities. For example, Figure 4 shows an event that was measured by Van Allen Probe A on 11 January 2013. A chorus wave is observed with a large spectral gap that exceeds $0.2 f_{ce}$ at the beginning (Figure 4b). This spectral gap shrank to a smaller one in a few minutes as the spacecraft travelled to locations of smaller f_{pe}/f_{ce} (Figure 4a) due to a decrease of the plasma density. The electron distribution in association with the large chorus spectral gap,

presented in Figure 4c, shows that $f(18^\circ)$ and/or $f(36^\circ)$ exceeded $f(90^\circ)$ from 0.3 keV to 1.3 keV, implying those electrons have undergone Landau resonant acceleration at latitudes at least up to $\sim 27^\circ$ (based on the empirical density model and dipole field model). The wide separation of the two anisotropic components led to the formation of a large chorus spectral gap. The electron distribution observed in association with a small chorus spectral gap in the low f_{pe}/f_{ce} region, shown in Figure 4d, indicates less pronounced parallel acceleration that extended to ~ 1.7 keV (using the criterion that $f(18^\circ)$ and/or $f(36^\circ)$ exceeded $f(90^\circ)$), corresponding to a Landau resonant acceleration at latitudes up to $\sim 20^\circ$.

We note that the upper limit of the chorus spectral gap in Figure 4 is above 0.5 f_{ce} , and the electron PSD plateaus are seen at velocities below 0.5 v_{Ae} . One possible explanation is that the electron PSD plateaus at lower energies were produced at nearby locations with larger f_{pe}/f_{ce} ratios and then drifted to the location of the satellite where the f_{pe}/f_{ce} is smaller.

4. Discussion

Although the linear instability theory can roughly explain the frequency of chorus spectral gaps, it has a few limitations that need to be considered. 1) The rising-tone spectral feature of chorus waves both at the lower- and upper- bands is believed to be generated due to nonlinear resonant interactions (e.g., *Omura et al.*, 2009; *Tao et al.*, 2020), which are not described by the linear theory regime. 2) As mentioned earlier, the measured electron anisotropy is usually smaller than needed to excite chorus waves according to linear theory, and in some upper-band chorus wave cases, the observed electron anisotropy is significantly smaller than that required by the linear theory for instability. 3) The electron distribution in Figure 2h shows electron isotropization up to 4.1 keV at 18° pitch angle, which corresponds to a parallel velocity of 0.84 v_{Ae} . If the electron distribution at $v_{\parallel} = 0.84 \, v_{Ae}$ is stable and does not excite chorus waves, a spectral gap down to 0.37 f_{ce} is expected according to the linear theory. However, the observed chorus spectral gaps stopped at 0.42 f_{ce} . It is possible that nonlinear interactions play a significant role in this process and generate waves in a wider range of frequencies than linear theory predictions. Nevertheless, we note that the linear theory can roughly and reasonably explain the wave source and the spectral gap formation.

As demonstrated by several case studies, the bandwidth of chorus spectral gaps is significantly influenced by the energy range of reduced electron anisotropy. However, variations in locations,

ambient magnetic field and plasma density may also influence the chorus gap width. Note that the spectral gap in the case of Figure 1a is wider than that in Figure 2a, although the electron PSD shown in Figure 2g shows a more pronounced plateau. One possible explanation is that as electrons with a PSD plateau inject inward, they undergo perpendicular acceleration due to the conservation of the first adiabatic invariant. At the new location, the overall distribution is anisotropized while the PSD plateau may still be apparent. If the electrons exhibit a substantial anisotropy around plateau energies, chorus waves with no gap or small gaps could still be generated.

269

270

271

272

273

274

275

276

277

278

279

280

281

282

283

284

285

286

287

288

289

290

291

292

293

294

295

296

297

298

299

Single-band chorus waves are often observed to be coexisting with banded chorus waves, and the coexistence observed off equator appears in morphologies different from that shown in Figure 1d. For instance, Figure 5a shows strong single-band chorus waves occurring intermittently and coexisting with weaker two-band chorus waves. Figure 5b shows an event in which some lowerband emissions are stronger than the upper-band, while other emissions are continuous across 0.5 f_{ce} . Figure 5c shows single-band chorus waves extending across 0.5 f_{ce} while some emissions are weaker at $0.5 f_{ce}$. Figures 5d and 5e show a case in which chorus waves were generally banded over the long term, while single-band chorus waves may occasionally occur over shorter time spans, for example a period of 20 seconds. The 3-minute averaged electron distribution associated with these waves (not shown) exhibits clear evidence of isotropization at Landau resonant energies and the resultant two anisotropic energy components. It is quite likely that the electron distributions vary rapidly on short timescales, but the 3-min averaged distributions cannot capture this variation. We note that although the HOPE instrument provides electron distribution at a cadence of 22 seconds, each sample contains a random noise due to low counting rates; therefore, we use 3-min averaged data to smooth out random noises (in the case of Figure 4, the electron PSD at energies of interest is high and the random noise is low, and we use 1-min averages). In addition, these coexisting single-band and banded chorus waves are observed away from equator (MLAT > 4.2°), and these waves may originate from different Lshells since they do not propagate strictly parallel to the magnetic field. Therefore, the observed electron population, even though it is projected to the equator, may not be completely representative of the source of those chorus waves. The conditions for excitation of single-band chorus waves, and the coexistence between single-band and banded chorus waves remain to be fully understood.

5. Conclusions

300

301

302

303

304

305

306

307

308

309

310

311

312

313

314

315

316

317

318

319

320

322

323

324

325

326

327

The present study compared a single-band chorus wave and a banded chorus wave measured closely in time by one of the Van Allen Probes spacecraft, and showed that the single-band chorus wave is associated with an anisotropic electron distribution without isotropization at Landau resonant energies, while the banded chorus waves are observed to be associated with an anisotropic electron population with a PSD plateau at 0.5 v_{Ae} . We then compared banded chorus waves with different spectral gap widths, and showed that chorus waves with wider gaps are associated with electron isotropization extending to higher energies. We suggest that a freshly injected anisotropic electron distribution can excite single-band chorus waves without a gap. Chorus waves generated early cause Landau resonant parallel acceleration at velocities around $0.5 v_{Ae}$. Landau resonance that extends to high latitudes isotropizes electrons at high energies. When electrons bounce back to the equator, the isotropized distribution suppresses the wave generation over a certain frequency range, and a more pronounced isotropization leads to a large chorus spectral gap. We use a beam population to model the electron parallel acceleration and utilize the linear instability theory to quantify the wave growth. We show that adding a beam to the anisotropic distribution leads to a chorus spectral gap. A beam with a larger density, which represents a

stronger parallel acceleration and a more pronounced isotropization, leads to a wider spectral gap.

As shown in the case of Figure 4c, chorus waves created a field-aligned population at hundreds of eV. Therefore, chorus waves provide an important mechanism for creating field-aligned

suprathermal electron populations observed in the magnetosphere (*Li et al.*, 2010), similar to hiss

wave-induced acceleration (*Li et al.*, 2019b).

Data Availability Statement

The waves, the magnetic field and the plasma density measured by Van Allen Probes are publicly available from https://emfisis.physics.uiowa.edu/Flight. The electron distributions measured by the HOPE instrument are publicly available from https://rbsp-ect.newmexicoconsortium.org/data_pub. The Van Allen Probe data analysis is carried out using the publicly available SPEDAS software (http://spedas.org).

Acknowledgement

328

JL, JB and XA acknowledge the NSF grant AGS-1923126 and NASA grant LWS-329 330 80NSSC20K0201 and 80NSSC21K0522. JL and JB acknowledge the grant DE-SC0010578 and 331 NASA grants 80NSSC18K1227 and NNX14AI18G. XA and JB acknowledge the NASA grant 332 80NSSC20K0917. WL acknowledges the NASA grants 80NSSC20K1506, 80NSSC19K0845, 333 and 80NSSC20K0698, NSF grant AGS-1847818, as well as the Alfred P. Sloan Research Fellowship FG-2018-10936. This work (including support for WK) is supported by RBSP-ECT 334 335 and EMFISIS funding provided by JHU/APL contract No. 967399 and 921647 under NASA's 336 prime contract No. NAS5-01072.

337 References

- Bortnik, J., U. S. Inan, and T. F. Bell (2006), Landau damping and resultant unidirectional
- propagation of chorus waves, Geophys. Res. Lett., 33, L03102, doi:10.1029/2005GL024553
- Burtis, W. J., and R. A. Helliwell (1969), Banded chorus—A new type of VLF radiation
- observed in the magnetosphere by OGO 1 and OGO 3, J. Geophys. Res., 74(11), 3002–3010,
- 342 doi:10.1029/JA074i011p03002.
- Coroniti, F. V., Scarf, F. L., Kennel, C. F., Kurth, W. S. and Gurnett, D. A. (1980), Detection of
- Jovian whistler mode chorus; Implications for the Io torus aurora. Geophys. Res. Lett., 7: 45-48.
- 345 doi:10.1029/GL007i001p00045
- Denton, R. E., Menietti, J. D., Goldstein, J., Young, S. L. & Anderson, R. R. (2004), Electron
- density in the magnetosphere. J. Geophys. Res. 109, A09215.
- Fu, X., et al. (2014), Whistler anisotropy instabilities as the source of banded chorus: Van Allen
- Probes observations and particle-in-cell simulations, J. Geophys. Res. Space Physics, 119, 8288–
- 350 8298, doi:10.1002/2014JA020364.
- Funsten, H. O. et al (2013). Helium, oxygen, proton, and electron (HOPE) mass spectrometer for
- the Radiation Belt Storm Probes mission. Space Sci. Rev. 179, 423-484.
- Gao, X., Lu, Q., Bortnik, J., Li, W., Chen, L., and Wang, S. (2016), Generation of multiband
- 354 chorus by lower band cascade in the Earth's magnetosphere, Geophys. Res. Lett., 43, 2343–
- 355 2350, doi:10.1002/2016GL068313.
- Gao, X., Chen, L., Li, W., Lu, Q., & Wang, S. (2019). Statistical results of the power gap
- between lower-band and upper-band chorus waves. Geophysical Research Letters, 46, 4098–
- 358 4105. https://doi.org/10.1029/2019GL082140.
- Gurnett, D. A. and A. Bhattacharjee (2005), Introduction to plasma physics: with space and
- 360 laboratory applications, Cambridge University Press
- Liu, K., Gary, S. P., & Winske, D. (2011). Excitation of banded whistler waves in the
- 362 magnetosphere. Geophys. Res. Lett., 38(14), L14108. https://doi.org/10.1029/2011GL048375

- Hospodarsky, G. B., T. F. Averkamp, W. S. Kurth, D. A. Gurnett, J. D. Menietti, O. Santolik,
- and M. K. Dougherty (2008), Observations of chorus at Saturn using the Cassini Radio and
- 365 Plasma Wave Science instrument, J. Geophys. Res., 113, A12206, doi:10.1029/2008JA013237.
- Kletzing, C., Kurth, W. S., Acuna, M., MacDowall, R. J., Torbert, R. B., Averkamp, T., ... Tyler,
- J. (2013). The electric and magnetic field instrument suite and integrated science (EMFISIS) on
- 368 RBSP. Space Science Reviews, 179(1-4), 127–181. https://doi.org/10.1007/s11214-013-9993-6.
- 369 Kennel, C. (1966), Low-frequency whistler mode, Physics of Fluids 9, 2190,
- 370 <u>http://dx.doi.org/10.1063/1.1761588</u>.
- Kurita, S., Y. Katoh, Y. Omura, V. Angelopoulos, C. M. Cully, O. Le Contel, and H. Misawa
- 372 (2012), THEMIS observation of chorus elements without a gap at half the gyrofrequency, J.
- 373 Geophys. Res., 117, A11223, http://dx.doi.org/10.1029/2012JA018076.
- Li, J., Bortnik, J., An, X., Li, W., Angelopoulos, V., Thorne, R. M., et al. (2019). Origin of two-
- 375 band chorus in the radiation belt of Earth. Nature Communications, 10(1), 4672.
- 376 https://doi.org/10.1038/s41467-019-12561-3
- Li, J., Ma, Q., Bortnik, J., Li, W., An, X., Reeves, G. D., et al. (2019). Parallel acceleration of
- 378 suprathermal electrons caused by whistler-mode hiss waves. Geophysical Research Letters, 46,
- 379 12,675–12,684. https://doi.org/10.1029/2019GL085562
- Li, J., Bortnik, J., Li, W., An, X., Lyons, L. R., Kurth, W. S., et al. (2022). Unraveling the
- formation region and frequency of chorus spectral gaps. Geophysical Research Letters, 49,
- 382 e2022GL100385. https://doi.org/10.1029/2022GL100385.
- Li, W., et al. (2010), THEMIS analysis of observed equatorial electron distributions responsible
- for the chorus excitation, J. Geophys. Res., 115, A00F11, https://doi.org/10.1029/2009JA014845.
- 385 Mauk, B. H., Fox, N. J., Kanekal, S. G., Kessel, R. L., Sibeck, D. G., & Ukhorskiy, A. (2013).
- 386 Science objectives and rationale for the Radiation BeltStorm Probes mission. Space Science
- 387 Reviews, 179(1-4), 3–27. https://doi.org/10.1007/s11214-012-9908-y.

- 388 Means, J. D. (1972). Use of the three-dimensional covariance matrix in analyzing the
- polarization properties of plane waves. Journal of Geophysical Research, 77, 5551–5559.
- 390 <u>https://doi.org/10.1029/JA077i028p05551</u>
- 391 Min, K., et al. (2015), Study of EMIC wave excitation using direction measurements, J. Geophys.
- 392 Res. Space Physics, 120, 2702–2719, doi:10.1002/2014JA020717.
- 393 Omura, Y., M. Hikishima, Y. Katoh, D. Summers, and S. Yagitani (2009), Nonlinear
- mechanisms of lower-band and upper-band VLF chorus emissions in the magnetosphere, J.
- 395 Geophys. Res., 114, A07217, doi:10.1029/2009JA014206.
- Omura, Y., Hsieh, Y. (2020), Generation of lower band and upper band whistler-mode chorus
- 397 emissions and associated electron acceleration in the inner magnetosphere, EGU General
- 398 Assembly 2020, https://doi.org/10.5194/egusphere-egu2020-2143
- Ratcliffe, H., & Watt, C. E. J. (2017). Self-consistent formation of a 0.5 cyclotron frequency gap
- 400 in magnetospheric whistler mode waves. J. Geophys. Res. Space Physics, 122(8), 8166–8180.
- 401 https://doi.org/10.1002/2017JA024399
- 402 Santolík, O., D. A. Gurnett, J. S. Pickett, M. Parrot, and N. Cornilleau-Wehrlin (2003), Spatio
- 403 temporal structure of storm-time chorus, J. Geophys. Res., 108(A7), 1278,
- 404 doi:10.1029/2002JA009791
- Schriver, D., et al. (2010), Generation of whistler mode emissions in the inner magnetosphere:
- 406 An event study, J. Geophys. Res., 115, A00F17, doi:10.1029/2009JA014932.
- Spence, H. E., G. D. Reeves, D. N. Baker, J. B Blake, M. Bolton, S. Bourdarie, A. H. Chan, S.
- 408 G. Claudepierre, J. H. Clemmons, J. P. Cravens, S. R. Elkington, J. F. Fennell, R. H. W. Friedel,
- 409 H. O. Funsten, J. Goldstein, J. C. Green, A. Guthrie, M. G. Henderson, R. B. Horne, M. K.
- 410 Hudson, J.-M. Jahn, V. K. Jordanova, S. G. Kanekal, B. W. Klatt, B. A. Larsen, X. Li, E. A.
- 411 MacDonald, I. R. Mann, J. Niehof, T. P. O'Brien, T. G. Onsager, D. Salvaggio, R. M. Skoug, S.
- S. Smith, L. L. Suther, M. F. Thomsen, and R. M. Thorne, Science Goals and Overview of the
- 413 Energetic Particle, Composition, and Thermal Plasma (ECT) Suite on NASA's Radiation Belt
- 414 Storm Probes (RBSP) Mission, Space Sci. Rev., DOI: 10.1007/s11214-013-0007-5, 2013.
- 415 Tao X, Zonca F, Chen L, Wu Y. 2020. Theoretical and numerical studies of chorus waves: A
- 416 review. Science China Earth Sciences, 63: 78–92, https://doi.org/10.1007/s11430-019-9384-6

- 417 Teng, Tao, X., & Li, W. (2019). Typical characteristics of whistler mode waves categorized by
- 418 their spectral properties using Van Allen Probes observations. Geophysical Research Letters, 46,
- 419 3607–3614. https://doi.org/10.1029/2019GL082161
- 420 Taubenschuss, U., O. Santolik, H. Breuillard, W. Li, and O. Le Contel, Poynting vector and
- wave vector directions of equatorial chorus, J. Geophys. Res. Space Physics, 121, 11,912–11,928
- 422 (2016), doi:10.1002/2016JA023389.

- Tsurutani, B. T., and E. J. Smith (1974), Postmidnight chorus: A substorm phenomenon, J.
- 424 Geophys. Res., 79(1), 118–127, doi:10.1029/JA079i001p00118.

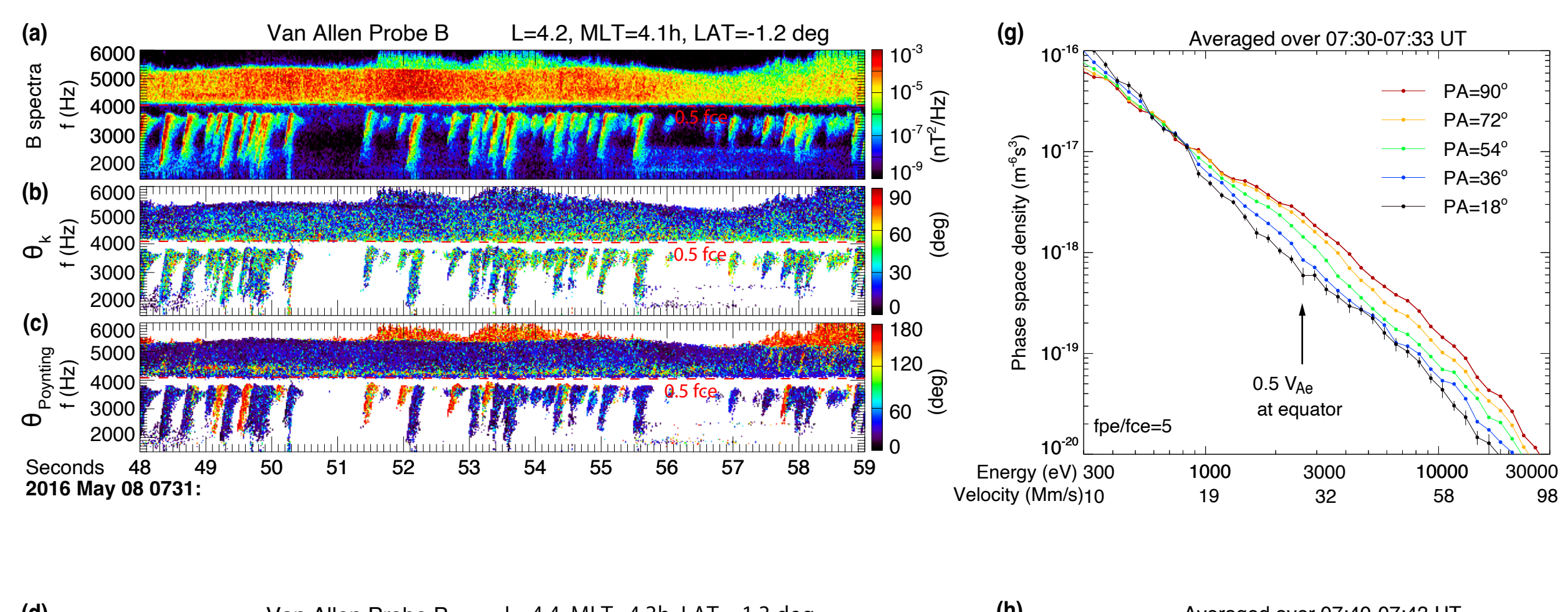
Figure Captions

426

- Figure 1. Observations of single-band and banded chorus waves and the associated electron PSD
- distributions. (a) The burst-mode wave magnetic spectral intensity measured at 07:31 UT,
- showing banded chorus waves. (b) The wave normal angle. (c) The Poynting flux angle. (d-f)
- The same as Figures 1a-1c, but measured at 07:42 UT, showing a mixture between single-band
- 431 chorus waves and banded chorus waves with tiny spectral gaps. (g-h) The electron PSD
- distribution averaged over 07:30-07:33 UT and 07:41-07:44 UT, respectively. The standard
- deviation of PSD for 18° pitch angle measured over 3 minutes is augmented in Figure 1g.
- Figure 2. Chorus waves with different gap widths and the associated electron PSD distributions.
- 435 (a) The wave spectral intensity measured at 09:26 UT, showing banded chorus waves with a
- small spectral gap. (b) The wave normal angle. (c) The Poynting flux angle. (d-f) The same as
- Figures 2a-2c, but measured at 09:33 UT, showing banded chorus waves with a large spectral
- gap. (g-h) The electron PSD averaged over 09:26-09:29 UT and 09:33-09:36 UT, respectively.
- 439 **Figure 3.** The impact of beam density to chorus gap width. (a) The electron PSD distribution
- 440 consisting of a cold isotropic distribution and a warm anisotropic distribution, color-coded for
- different pitch angles. (b) The electron PSD distribution after being added a weak beam
- 442 (n_b=0.002 cm⁻³), representing a weak Landau resonant acceleration. (c) The electron PSD after
- being added a stronger beam (n_b=0.004 cm⁻³), representing an enhanced Landau resonant
- acceleration extending to more energies. (d-f) The linear growth rates of chorus waves from
- three different distributions, respectively, color-coded for various wave normal angles of chorus.
- 446 Figure 4. Banded chorus waves and electron distributions in the 11 January 2013 event. (a) The
- 447 f_{pe}/f_{ce} ratio. (b) The wave magnetic spectral intensity. (c-d) The 1-minute averaged electron PSD
- distributions at 11:50 UT and 11:56 UT, respectively, color-coded for various pitch angles.
- 449 Figure 5. Different forms of mixture between single-band and banded chorus waves. (a) Strong
- 450 single band chorus waves coexist with weaker banded chorus waves. (b) Some lower-band
- emissions are stronger than the upper-band by 2-3 orders, while other emissions are continuous
- across $0.5 f_{ce}$ without a significant intensity decrease. (c) Some chorus emissions are single-
- banded, while other emissions are significantly weaker at 0.5 f_{ce} . (d) and (e), A case in which

- 454 chorus waves were generally banded over half an hour, while single-band chorus waves
- occasionally occur over a period of 20 seconds.

Figure	1.
--------	----



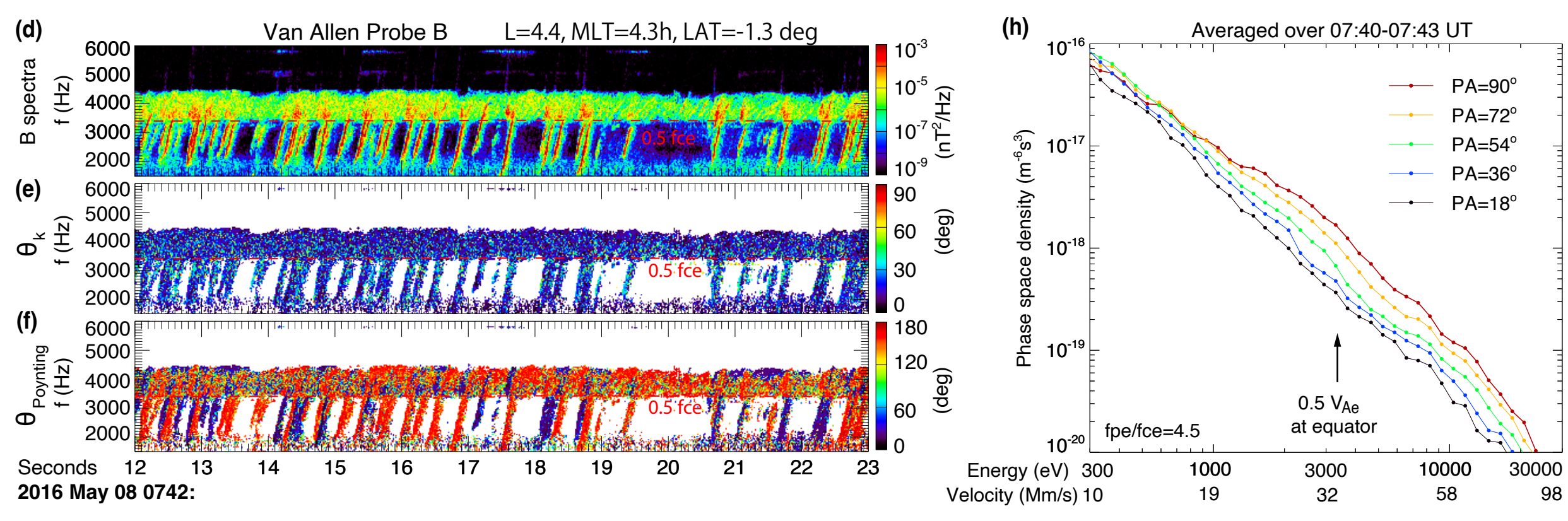
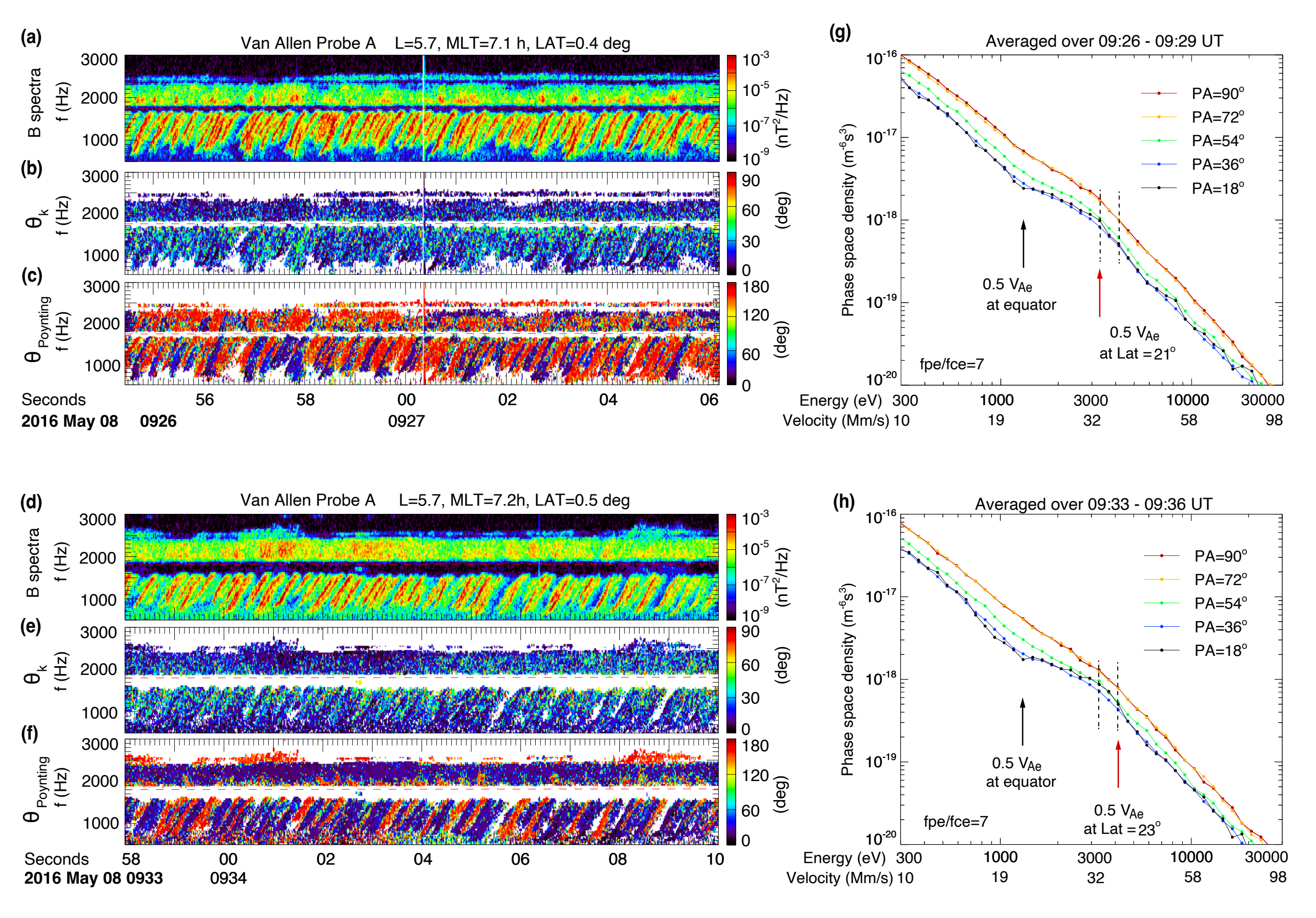


Figure	2.
--------	----



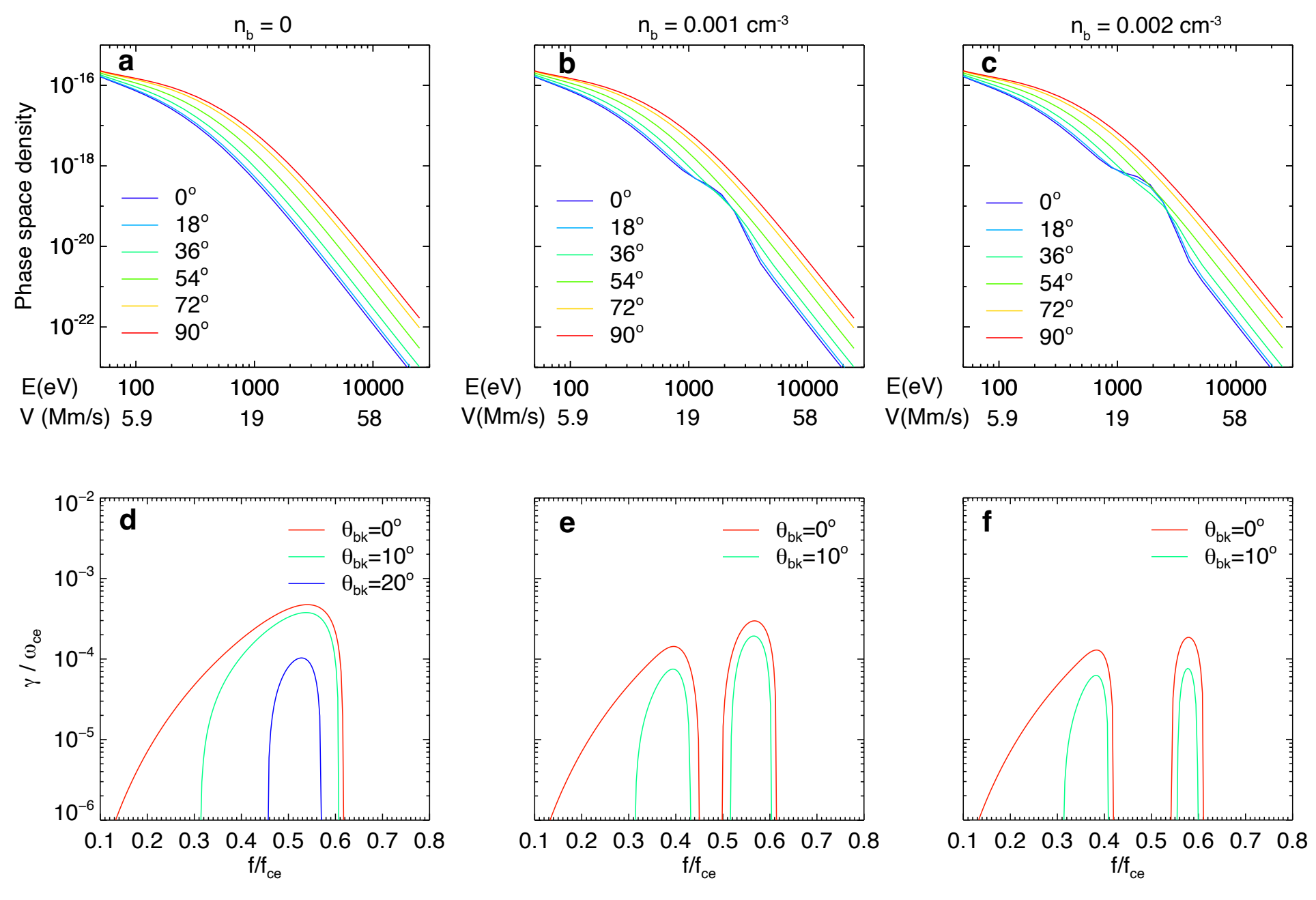


Figure 4.	
-----------	--

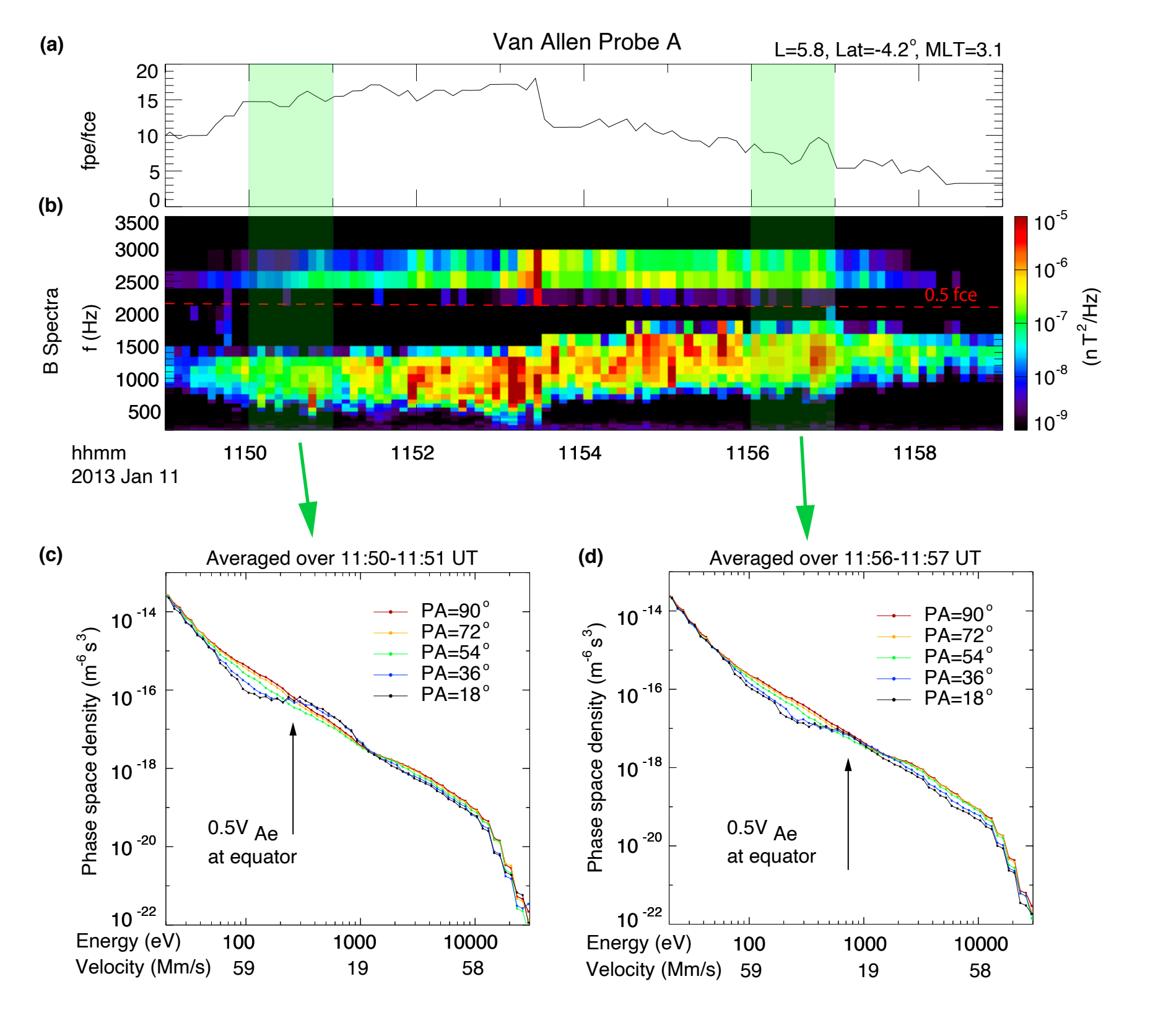


Figure 5.	
-----------	--

